Indentation creep of a Ti-based metallic glass

Huang, Y.j.; Chiu, Y.l.; Shen, J.; Chen, J.j.j.; Sun, J.f.

DOI:
10.1557/jmr.2009.0106

Document Version
Early version, also known as pre-print

Citation for published version (Harvard):
Huang, YJ, Chiu, YL, Shen, J, Chen, JJJ & Sun, JF 2009, 'Indentation creep of a Ti-based metallic glass', *Journal of Materials Research*, vol. 24, no. 03, pp. 993-997. https://doi.org/10.1557/jmr.2009.0106

Indentation creep of a Ti-based metallic glass

Y.J. Huang
School of Materials Science and Engineering, Harbin Institute of Technology, Harbin 150001, China; and Department of Chemical and Materials Engineering, University of Auckland, Auckland 1142, New Zealand

Y.L. Chiu[a)]
Department of Chemical and Materials Engineering, University of Auckland, Auckland 1142, New Zealand; and Department of Metallurgy and Materials, University of Birmingham, Edgbaston B15 2TT, United Kingdom

J. Shen[b)]
School of Materials Science and Engineering and Micro/Nano Technology Research Center, Harbin Institute of Technology, Harbin 150001, China

J.J.J. Chen
Department of Chemical and Materials Engineering, University of Auckland, Auckland 1142, New Zealand

J.F. Sun
School of Materials Science and Engineering, Harbin Institute of Technology, Harbin 150001, China

(Received 30 July 2008; accepted 31 October 2008)

In this work, the time-dependent plastic deformation behavior of $Ti_{40}Zr_{25}Ni_3Cu_{12}Be_{20}$ bulk and ribbon metallic glass alloys was investigated using a nanoindentation technique at room temperature with the applied load ranging from 5 to 100 mN. The stress exponent n, defined as $\dot{\varepsilon} = A\sigma^n$, has been derived as a measure of the creep resistance. It was found that the measured stress exponent increases rapidly with increasing indentation size, exhibiting a positive size effect. The size effect on the stress exponent n obtained from the bulk sample is more pronounced than that obtained from the ribbon sample. The deformation mechanism involved will be discussed.

I. INTRODUCTION

Due to the high-strength, high elastic limit and excellent corrosion resistance, bulk metallic glasses (BMGs) have attracted increasing interest in the research community.[1–3] However, BMGs often have limited plasticity when deformed at temperatures below their glass transition temperatures.[4,5] Depth-sensing nanoindentation is an ideal technique to probe the mechanical properties of glassy alloys from a small volume.[6–8] During indentation, the applied load can be controlled at a constant value, whereas the penetration of the indenter tip into the sample surface is continuously recorded. This is often called the constant-load indentation creep test, and it has been widely used to study the time-dependent plasticity (creep) of crystalline materials.[9–12] The stress exponent, n, of steady-state creep can be derived from the constant-load indentation tests.[9,10,13,14] However, nanoindentation creep studies of glassy alloys are rare.[15–17]

In this work, the time-dependent deformation behavior of Ti-based metallic glass has been studied using the nanoindentation technique. Our experiments have shown a size effect on the stress exponent n, and this effect is more significant on the ribbon sample, and the stress exponent measured from the bulk metallic glass sample is larger than that measured from the ribbon sample.

II. EXPERIMENTAL PROCEDURE

Alloy ingots with nominal composition of $Ti_{40}Zr_{25}Ni_3Cu_{12}Be_{20}$ (at.%) were prepared by arc melting a mixture of pure elements in a Ti-gettered argon atmosphere. Bulk glassy samples (10 mm in diameter and 60 mm in length) were obtained by drop cast into a copper mold. Ribbon samples (40 μm in thickness and 2 mm in width) were produced from the same master alloy by using the conventional single-roller spinning technique. The specimens were mechanically polished down to 1 μm before nanoindentation experiments were conducted at room temperature on an MTS Nano Indenter XP system (Oak Ridge, TN) using a Berkovich indenter. Fused silica was used as a standard sample for the initial tip calibration procedure. Before each test, efforts were made to minimize

Address all correspondence to these authors.
[a)]e-mail: y.chiu@bham.ac.uk
[b)]e-mail: junshen@hit.edu.cn
DOI: 10.1557/JMR.2009.0119

possible effects such as noise and vibration on the measurement. After the creep holding period, the applied load was decreased to 10% of the maximum load and held for 100 s to correct the thermal drift. Constant-load indentation creep tests were carried out with a constant loading rate of 0.1 mN s^{-1} to different peak loads of 5, 10, 35, 50, and 100 mN. In the tests, the peak load was held for 2000 s and then unloaded 0.1 mN s^{-1}. At least six indentation tests were performed under each test condition. The standard deviation was found to be less than 10%.

III. RESULTS AND DISCUSSION

Figure 1(a) shows load-displacement nanoindentation curves under load control mode, for the tests on the bulk metallic glass sample. It can be seen that all of the loading curves overlapped and the associated serrated flow, typical of metallic glass alloys. The serration (i.e., pop-in) becomes more obvious at larger loads on the loading curve, consistent with literature on nanoindentation studies on BMG alloys.[7] The recent uniaxial test of a Zr-based BMG by Jiang et al. further confirms that the serration is a result of shear bands.[18] They also noticed that the serration magnitude recorded is associated with the applied strain rate in that high strain rate promotes serration of small magnitude, whereas low strain rate produces large serration. In the present study, we used constant-rate loading (i.e., $\dot{P}$= constant), the indentation strain rate ($\sim\dot{P}/P$) thus continuously decreases with increasing load P. Therefore, our observation, where less dense but more obvious serrations (pop-ins) occur at large load (i.e., low strain rate) on the loading curve, agrees with that reported by Jiang et al.[18]

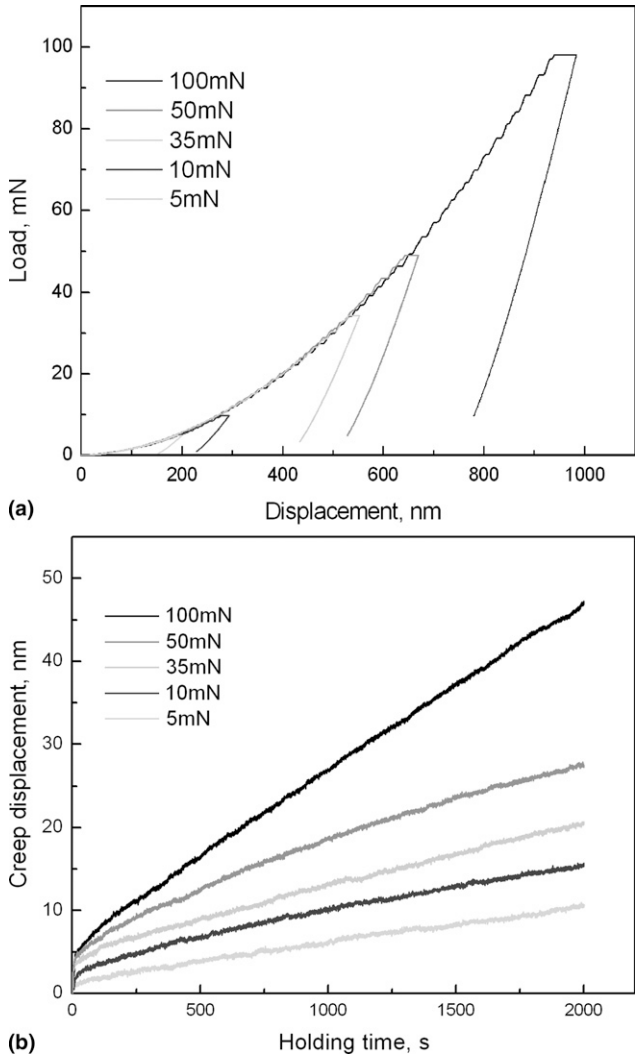

FIG. 1. (a) Typical load-displacement curves of Ti-based bulk glass sample under different peak loads at room temperature and (b) the corresponding creep displacement during load hold. The displacement axis was reset to show only the creep displacement, and time was reset to zero at the beginning of the hold period to facilitate comparison.

During the peak load holding, the indenter continues to penetrate into the test sample with time. Figure 1(b) shows the penetration of the indenter tip into the sample surface (i.e., creep displacement) during the peak load holding against the holding time. The magnitude of the total creep displacement during the peak load holding is strongly load dependent, i.e., larger peak load causes larger penetration. The creep displacement increases but at a decreasing rate, and it becomes almost linear with regard to the holding time. The total creep displacements are in the range of 10∼50 nm for different holding loads. The consistent load dependency observed and the different creep deformation magnitude observed between the bulk sample and the ribbon sample suggest that thermal drift is unlikely to have a dominant effect on the displacement measurement.

Following Johnson's expanding cavity model[19] and the calculation of Bower et al.,[20] a self-similar stress/stain field can be assumed underneath a self-similar indenter. We further assume that steady-state creep has been reached during the creep holding and use the following procedure to derive the stress exponent n, as defined in the conventional power-law creep, which writes[19,20]

$$\dot{\varepsilon} = A\sigma^n \quad , \tag{1}$$

where $\dot{\varepsilon}$ is the strain rate, σ is the applied stress, and A is a temperature-dependent material constant. The stress exponent that often provides useful indication on the creep mechanisms involved can then be derived as $n = \partial(\ln\dot{\varepsilon})/\partial(\ln\sigma)$. In indentation, the strain-rate and stress can be written following the scaling relations:

$$\dot{\varepsilon} \sim \dot{h}/h\,\sigma \sim P/24.5h^2 \quad , \tag{2}$$

where P is the applied load, h is the instantaneous indentation depth, and the displacement rate is $\dot{h} = dh/dt$[10], which can be obtained by fitting the creep displacement-holding time curve at a constant load using an empirical equation[13]:

$$h(t) = h_0 + a(t - t_0)^b + kt \quad , \tag{3}$$

where h_0, a, b, t_0, and k are fitting constants. An example of the experimental data and fitted curve is shown in Fig. 2(a), where the total creep displacement was 15.5 nm. Equation (3) was found to fit the creep curves very well.

Figure 2(b) shows the *log(strain rate) versus log (stress)* relation of the bulk glass sample for hold period of 2000 s at 10 mN. The slope of the decreases rapidly with the holding time (i.e., where the stress decreases) and then gradually become constant at the end of the holding period. The slope at the left hand of the curve (i.e., 2.6), which corresponds to the end of the holding period, was taken to be the stress exponent n for the peak load. Figure 3 shows the variation of n values as a function of the contact depth for the Ti-based bulk metallic glass samples. For the purpose of comparison, the n values as a function of the peak loads for ribbon sample were also presented in Fig. 3. It is clear that as peak load increases from 5 to 100 mN (i.e., as the contact depth increases from 188.8 to 939.1 nm), the n value increases from 1.4 to 5.1 for the bulk metallic glass sample, and in the case of the ribbon sample, the n value increases from 0.67 to 1.75. The stress exponent exhibits clear size-dependent indentation. At the same time, the stress exponent obtained from the ribbon sample is consistently smaller than that obtained from the bulk sample under the same loading conditions. This further confirms that the thermal drift is not dominant in the creep displacement, because otherwise one would not expect the consistency observed at different loads and samples.

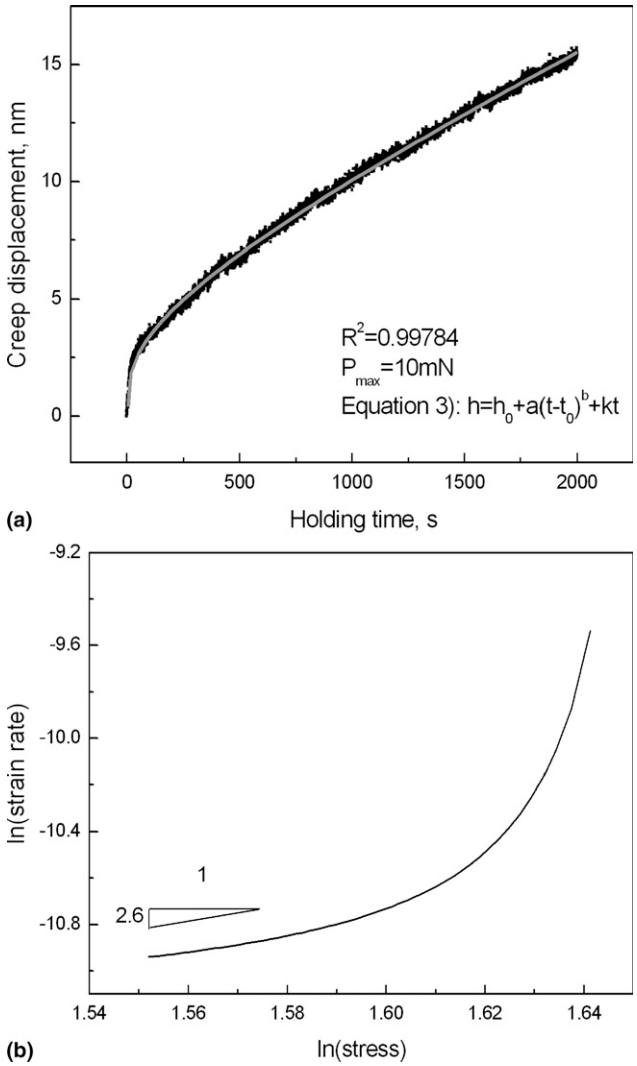

FIG. 2. (a) Creep response of Ti-based bulk glass sample for hold period of 2000 s at 10 mN [Data points show experimental results, and the solid line shows the fitted response according to Eq. (3)] with h_0 = 277.01436 ± 0.13059, a = 0.8401 ± 0.07576, b = 0.3241 ± 0.011, and k = 0.0042 ± 0.00004. (b) The corresponding ln(strain rate) versus ln(stress) plot.

A few studies have reported the indentation size effect on the n values measured in the indentation creep for crystalline materials and oxide glass materials.[13,14,21] For pure Al polycrystalline and Ni_3Al single crystal, the creep mechanism changes from linear diffusional flow to a climb-controlled and eventually glide-controlled process as the indentation size gets larger.[13] In the case of tin-antimony alloys, a transition from climb-controlled creep at low stress to viscous glide-controlled creep at high stresses was observed during indentation creep.[21] A strong size effect on the indentation creep response was also found in as-deposited plasma-enhanced chemical vapor deposition silicon oxide-thin films, where the creep mechanism was depicted using defect flowing.[14] However, to date, the indentation size effect on the stress exponent of indentation creep for glassy alloy has not been reported.

The plastic deformation mechanisms of metallic glass have been proposed based on the concept of diffusive

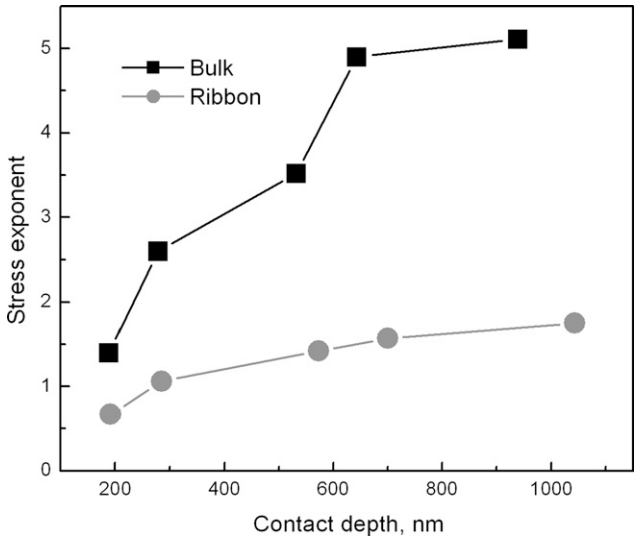

FIG. 3. Steady-state stress exponent, n, as a function of the contact depths for Ti-based ribbon and bulk glass samples.

atomic jump (developed by Turnbull and coworkers[22]) and applied to the case of glass deformation (developed by Spaepen[23]) or that of "shear transformation zone" (STZ; proposed by Argon[24]) (see the discussion by Falk and Langer[25] and the recent review by Schuh et al.[26]). STZ is considered as the basic shear unit, which consists of a large, free volume site with immediate adjacent atoms. These atomic-scale STZs collectively deform under an applied shear stress to produce shear banding.[24–26] The size-dependent indentation of the stress exponent observed is interesting in the present work. During nanoindentation tests, plastic deformation is confined within a small volume of material associated with a nonuniform stress and strain field of strong gradient.[27] At small indentation depth, the strain gradient is significantly larger than that at large indentation depth. The strain gradient exerts a crucial role in determining the plastic flow of materials during nanoindentation.[28,29] It was presumed that the strain gradient would lead to an extra imbalance among the STZs and increase the rate at which the shear bands form and relax underneath the indenter of metallic glass.[14] Because the volume involved in the deformation is smaller, the shear bands generated at shallow depths should generally be much smaller than those generated at larger depths. The evolution of shear band patterns from small and semicircular shape to secondary and tertiary shear bands with increasing load during indentation tests has been observed for a Zr-based glassy alloy.[30] At steady state, atomic diffusion may be enhanced as a result of the higher rate of dynamic equilibrium in the rearrangement of STZs.[14] As such, the numerous smaller shear bands in the specimen may collectively exhibit a more macroscopically viscous-like flow behavior, whereas the localization in few shear banding at larger indentation size results in more inhomogeneous plastic flow. This is consistent with the lower stress exponent at smaller indentation size, as shown in Fig. 3.

According to the STZ theory,[24] a large n value indicates the inhomogeneous plastic flow of the material. It is natural to envisage that the structure (e.g., the level of free volume) of a metallic glass is dependent on the cooling rate of glass formation.[31] In fast-cooled glass, more sites with higher free volume are more easily associated with the existence of STZs. This may in turn facilitate the shear band initiation by either decreasing the required activation energy as looser structure eases the atomic jump and/or atomic rearrangement in the STZ or rendering more possible STZs. Compared with the results from the bulk metallic glass sample, more sites with higher free volume are created in the ribbon sample due to a higher cooling rate used,[31] easing the shear banding and leading to a more homogeneous flow, thus resulting in smaller n values. In other words, the plastic deformation of open glass structure tends to be more homogeneous.

Plastic flow patterns generated during indentation creeps of BMG will help to understand the creep mechanisms involved, e.g., to answer whether it is the shear band nucleation or the propagation of existent shear bands that accounts for the creep deformation. To isolate the creep-induced plastic flow patterns from that introduced in the preceding loading process, it is essential to image the plastic flow patterns before the creep holding; this method is possible using the bonded interface technique. The interface-bonded sample will be indented without the holding period at the maximal load and then unloaded, debonded, and imaged.[18] However, after the imaging, the interface has to be rebonded exactly as the previous bonding and then a second indentation test with creep holding has to be done on the exact indent position, to the same maximal load as the first test, and then the plastic flow patterns can be imaged at the end of the test. To rebond the interface exactly the same and to make the second indentation test on an interface-rebonded sample at the exact position as the first test remains a challenge. To this end, a set of indentation creep tests were performed (on the same nanoindentation machine) using a flat punch indenter on the focused ion beam machined micropillars of a Zr-based BMG with composition similar to that reported by Jiang et al.[18] The shear band patterns on the surface of the column have been imaged using SEM, and the results showed that the creep observed was caused by propagation and/or branching of existing shear bands, rather than the nucleation of shear bands.[32] According to Jiang et al.,[18] the spatial shear band distribution is closely related to the temporality of shear banding such that, in nanoindentation, a low strain rate promotes the temporal heterogeneity of shear banding and vice versa for a high strain rate. During indentation loading, many fine and spatially homogenous shear bands are generated at the low load level (i.e., high strain rate), and as the load gradually increases, the strain rate decreases, thus coarse and localized shear bands are generated. The localized coarse shear bands effectively promote the following creep deformation by further branching and/or propagation, resulting in a larger stress exponent value, as shown in Fig. 3.

During an indentation test, the stress/strain field underneath an indenter is not homogeneous, and the volume of material involved expands as the indenter penetrates into the testing material.[33] The assumption of steady-state creep in an indentation holding test has been discussed by Bower et al.[20] Although deformation behavior of amorphous alloys may be affected by strain softening and/or structural relaxation, they have homogeneous structure, which is a significant advantage over the heterogeneous structure associated with crystalline materials for time-dependent deformation studies. For example, the microstructure characteristics such as interface and interphase are important factors that influence the creep resistance of

the testing crystalline materials. These microstructure characteristics are often temporal and spatial dependent. Using amorphous alloys for time-dependent creep study simplifies the microstructure concern.

Note that, due to the inhomogeneous strain field and expanding volume, the stress exponent value derived from the present indentation creep may be different from that measured in a conventional tensile/compression creep test. Nonetheless, nanoindentation provides a straightforward method to evaluate the time-dependent deformation behavior of small metallic glassy alloys. However, a better understanding of the indentation creep mechanisms, such as the indentation size dependence and the cooling rate dependence observed in the present study of Ti-based BMG alloys, requires further experimental investigations, such as elevated temperature indentation creep.

IV. CONCLUSION

In summary, indentation creep tests on $Ti_{40}Zr_{25}Ni_3Cu_{12}Be_{20}$ metallic glass have been performed by constant load holding at room temperature. The stress exponent value measured on both bulk and ribbon glass samples increases with the increasing holding load, showing a positive indentation size dependence. The ribbon sample, which was prepared with a faster cooling, has smaller n values than that measured on a bulk glass sample, indicating a more homogeneous flow behavior.

ACKNOWLEDGMENTS

The financial support from the Program for New Century Excellent Talents in University (China), the National Natural Science Foundation of China (NSFC) under Grant Nos. 50771040 and 10732010, the Hi-Tech Research and Development Program of China (Project No. 2007AA03Z518), and a grant from the University of Auckland, New Zealand (Project No. 9217/3609144) are gratefully acknowledged.

REFERENCES

1. A. Inoue: Stabilization of metallic supercooled liquid and bulk amorphous alloys. *Acta Mater.* **48,** 279 (2000).
2. W.L. Johnson: Bulk glass-forming metallic alloys: Science and technology. *MRS Bull.* **24,** 42 (1999).
3. W.H. Wang, C. Dong, and C.H. Shek: Bulk metallic glasses. *Mater. Sci. Eng., R* **44,** 45 (2004).
4. A.R. Yavari, J.J. Lewandowski, and J. Eckert: Mechanical properties of bulk metallic glasses. *MRS Bull.* **32,** 635 (2007).
5. Z.F. Zhang, G. He, J. Eckert, and L. Schultz: Fracture mechanisms in bulk metallic glassy materials. *Phys. Rev. Lett.* **91,** 045505 (2003).
6. W.C. Oliver and G.M. Pharr: An improved technique for determining hardness and elastic modulus using load and displacement sensing indentation experiments. *J. Mater. Res.* **7,** 1564 (1992).
7. C.A. Schuh and T.G. Nieh: A nanoindentation study of serrated flow in bulk metallic glasses. *Acta Mater.* **51,** 87 (2003).
8. J-J. Kim, Y. Choi, S. Suresh, and A.S. Argon: Nanocrystallization during nanoindentation of a bulk amorphous metal alloy at room temperature. *Science* **295,** 654 (2002).
9. M.J. Mayo and W.D. Nix: A micro-indentation study of superplasticity in Pb, Sn, and Sn-38 wt% Pb. *Acta Metall.* **36,** 2183 (1988).
10. B.N. Lucas and W.C. Oliver: Indentation powder-law creep of high-purity Indium. *Metall. Mater. Trans. A* **30,** 601 (1999).
11. A.C. Fischer-Cripps: A simple phenomenological approach to nanoindentation creep. *Mater. Sci. Eng., A* **385,** 74 (2004).
12. W.B. Li and R. Warren: A model for nano-indentation creep. *Acta Metall.* **41,** 3065 (1993).
13. H. Li and A.H.W. Ngan: Size effects of nanoindentation creep. *J. Mater. Res.* **19,** 513 (2004).
14. Z.Q. Cao and X. Zhang: Nanoindentation creep of plasma-enhanced chemical vapor deposited silicon oxide thin films. *Scr. Mater.* **56,** 249 (2007).
15. A. Concustell, J. Sort, A.L. Greer, and M.D. Baró: Anelastic deformation of a $Pd_{40}Cu_{30}Ni_{10}P_{20}$ bulk metallic glass during nanoindentation. *Appl. Phys. Lett.* **88,** 171911 (2006).
16. W.H. Li, K. Shin, C.G. Lee, B.C. Wei, T.H. Zhang, and Y.Z. He: The characterization of creep and time-dependent properties of bulk metallic glasses using nanoindentation. *Mater. Sci. Eng., A* **478,** 371 (2008).
17. B.C. Wei, T.H. Zhang, W.H. Li, D.M. Xing, L.C. Zhang, and Y.R. Wang: Indentation creep behavior in Ce-based bulk metallic glasses at room temperature. *Mater. Trans.* **46,** 2959 (2005).
18. W.H. Jiang, G.J. Fan, F.X. Liu, G.Y. Wang, H. Choo, and P.K. Liaw: Spatiotemporally inhomogeneous plastic flow of a bulk-metallic glass. *Int. J. Plast.* **24,** 1 (2008).
19. K.L. Johnson: *Contact Mechanics* (Cambridge University Press, Cambridge, UK, 1985).
20. A.F. Bower, N.A. Fleck, A. Needleman, and N. Ogbonna: Indentation of a power law creeping solid. *Proc. R. Soc. London, Ser. A* **441,** 97 (1993).
21. R.J. McCabe and M.E. Fine: Creep of tin, Sb-solution-strengthened tin, and SbSn-precipitate-strengthened tin. *Metall. Mater. Trans. A* **33,** 1531 (2002).
22. D. Turnbull and M.H. Cohen: On the free-volume model of the liquid-glass transition. *J. Chem. Phys.* **52,** 3038 (1970).
23. F. Spaepen: A microscopic mechanism for steady state inhomogeneous flow in metallic glasses. *Acta Metall.* **25,** 407 (1977).
24. A.S. Argon: Plastic deformation in metallic glasses. *Acta Metall.* **27,** 47 (1979).
25. M.L. Falk and J.S. Langer: Dynamics of viscoplastic deformation in amorphous solids. *Phys. Rev. E* **57,** 7192 (1998).
26. C.A. Schuh, T.C. Hufnagel, and U. Ramamurty: Mechanical behavior of amorphous alloys. *Acta Mater.* **55,** 4067 (2007).
27. W.D. Nix and H. Gao: Indentation size effects in crystalline materials: A law for strain gradient plasticity. *J. Mech. Phys. Solids* **46,** 411 (1998).
28. D.C.C. Lam and A.C.M. Chong: Model and experiments on strain gradient hardening in metallic glass. *Mater. Sci. Eng., A* **318,** 313 (2001).
29. F. Yang, K. Geng, P.K. Liaw, G. Fan, and H. Choo: Deformation in a $Zr_{57}Ti_5Cu_{20}Ni_8Al_{10}$ bulk metallic glass during nanoindentation. *Acta Mater.* **55,** 321 (2007).
30. H. Zhang, X. Jing, G. Subhash, L.J. Kecskes, and R.J. Dowding: Investigation of shear band evolution in amorphous alloys beneath a Vickers indentation. *Acta Mater.* **53,** 3849 (2005).
31. Y.J. Huang, J. Shen, and J.F. Sun: Bulk metallic glasses: Smaller is softer. *Appl. Phys. Lett.* **90,** 081919 (2007).
32. Y.L. Chiu: unpublished results.
33. R. Goodall and T.W. Clyne: A critical appraisal of the extraction of creep parameters from nanoindentation data obtained at room temperature. *Acta Mater.* **54,** 5489 (2006).